Dual-Color Fluorescence-Burst Analysis to Probe Protein Efflux through the Mechanosensitive Channel MscL

Geert van den Bogaart,* Victor Krasnikov,[†] and Bert Poolman*

*Biochemistry Department and [†]Ultrafast Laser and Spectroscopy Laboratory, Groningen Biomolecular Science and Biotechnology Institute & Materials Science Centre[plus], University of Groningen, Groningen, The Netherlands

ABSTRACT   The mechanosensitive channel protein of large conductance, MscL, from *Escherichia coli* has been implicated in protein efflux, but the passage of proteins through the channel has never been demonstrated. We used dual-color fluorescence-burst analysis to evaluate the efflux of fluorescent labeled compounds through MscL. The method correlates the fluctuations in intensity of fluorescent labeled membranes and encapsulated (macro)molecules (labeled with second fluorophore) for each liposome diffusing through the observation volume. The analysis provides quantitative information on the concentration of macro-molecules inside the liposomes and the fraction of functional channel proteins. For MscL, reconstituted in large unilamellar vesicles, we show that insulin, bovine pancreas trypsin inhibitor, and other compounds smaller than 6.5 kDa can pass through MscL, whereas larger macromolecules cannot.

INTRODUCTION

Mechanosensitive channels (MS) are found in bacteria, fungi, plants, and animals and play a vital role in cell physiology (1). Upon a dilution of the external osmolyte concentration, bacterial cells eject cytoplasmic molecules, including ions, metabolites (2), and possibly proteins (3). For instance, *Escherichia coli* releases a subset of proteins, up to 10% of total protein content, when cells are dispersed in water (4). At least part of the cytoplasmic molecules released has been attributed to membrane channel proteins gated by mechanical forces (5). For a basic understanding of protein release by microorganisms and for biomedical applications, it is important to establish whether channel proteins of large conductance can facilitate the passage of macromolecules. For instance, liposomes containing mechanosensitive channels have been proposed as drug delivery vehicles for the controlled release of therapeutic peptides and proteins (6). In the case of the MS channel of large conductance (MscL) from *E. coli*, the protein or membrane environment has been engineered to allow the channel to open and close in response to light or pH (7,8).

MscL is the biophysically and biochemically best characterized MS channel protein and has a large conductance of 2.5–4 nS (1). On the basis of the crystal structure of the homologous MscL protein from *Mycobacterium tuberculosis* (9) and a protein fusion study (10), MscL is predicted to form a pentamer. From molecular modeling (11,12), patch-clamp studies (11), and in vivo and in vitro flux measurements (5,13–15), the diameter of the pore of MscL has been estimated to be between 30 and 40 Å. This diameter should be sufficient for the release of small proteins, but it is not known how large a molecule can actually pass through MscL (4,5,8,11,14,15).

Here, we used dual-color fluorescence-burst analysis, to monitor efflux of a broad range of (macro)molecules through a membrane pore. This analysis is based upon the fluorescent DiO labeling of MscL-containing liposomes and encapsulating macromolecules labeled with a second fluorophore Alexa fluor 633 (Fig. 1). The fluorescent lipid analog DiO and Alexa fluor 633 have nonoverlapping excitation and emission spectra and can be detected separately. For both labels, the fluorescence intensity fluctuations, resolving from the liposome diffusing through the observation volume of a confocal microscope, are correlated with each other. To activate MscL, a cysteine was engineered at the constriction site of the pore (G22C) for labeling with thiol-specific reagents. MscL (G22C) is pushed open when a charge is introduced at the Cys-22 site (16). Labeling of MscL G22C with MTSET introduces five (positively charged) choline moieties at the constriction site of the pore (8), whereas MTSES introduces (negatively charged) sulfonaethyl moieties (16).

A set of peptides and stably folded proteins were chosen as substrates for efflux through MscL (Table 1). The number of DiO molecules per liposome is independent of the state (open or closed) of MscL, whereas the number of Alexa fluor 633-labeled macromolecules does depend on this state. With MscL in the open state, the labeled molecules, depending on their size, might be released. When DiO-labeled liposomes, with encapsulated Alexa fluor 633-labeled molecules, diffuse through the observation volume of the confocal microscope, the DiO and the Alexa fluor 633 signals correlate (Fig. 1 *a*). If the macromolecules are small enough to efflux through MscL, opening of MscL G22C by chemical modification with MTSET or MTSES (16) will reduce this correlation (Fig. 1 *b*). Molecules smaller than bovine pancreas trypsin inhibitor ((BPTI) molecular weight of 6511) effluxed through MscL, whereas histidine-containing protein ((HPr) molecular weight
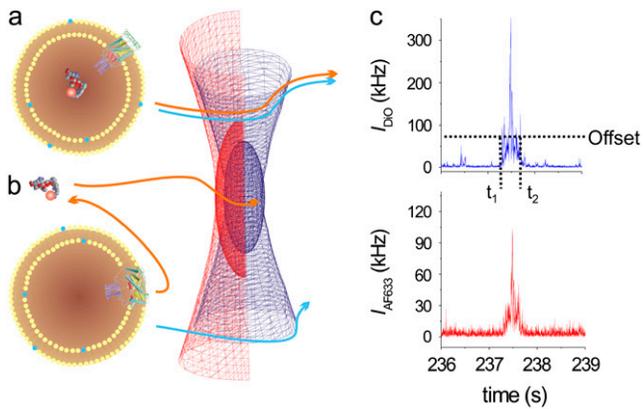
FIGURE 1 Principle of the dual-color fluorescence-burst analysis. (a) The focal geometry of a two-channel confocal microscope and diffusion of DiO-labeled liposomes (blue), containing Alexa fluor 633-labeled macromolecules (red). Note that the diffusion of the two fluorophores coincides. (b) Like panel a but after opening of MscL and release of the macromolecules. Note that the diffusion no longer coincides. (c) Fluorescence count traces resulting from the diffusion of DiO-labeled liposomes (blue trace, I_{DiO}) with Alexa fluor 633-labeled glutathione encapsulated (lower trace, I_{AF633}). Between t_1 and t_2 the intensity of the DiO signal is above the offset.

of 9119) and larger molecules did not. These observations were confirmed using fluorescence correlation spectroscopy (FCS). Furthermore, we show that only a fraction of the MscL channel molecules participated in the protein transport across the membrane.

METHODS

MscL purification and reconstitution in liposomes

MscL G22C (16) was expressed in the *E. coli mscL*-knockout strain PB104 (17) using vector pB10b (18). Cells were grown to midexponential growth phase (optical density at 660 nm of 0.5) and expression of *mscL* was induced by adding 1 mM isopropyl-β-D-thiogalactopyranoside (IPTG). Membrane vesicles were then prepared by rupturing the cells with a high-pressure homogenizer (Kindler Maschinen AG, Zürich, Switzerland) and solubilized by 3% octyl-β-glucoside. MscL was purified using nickel affinity chromatography as described previously (19).

TABLE 1   Size and dimensions of the macromolecules

Substrate	Molecular weight*	D ($\mu m^2 s^{-1}$)[†]	Dimensions (Å)[‡]	MscL[§]
Glutathione	307	135	$14 \times 3 \times 5$	+
Bradykinin R9C	1006	115	$24 \times 13 \times 11$	+
Insulin	5733	100	$31 \times 29 \times 24$	+
BPTI	6511	95	$23 \times 21 \times 31$	+
HPr	9119	80	$32 \times 32 \times 33$	−
Thioredoxin	11,502	75	$25 \times 30 \times 35$	−
α-Lactalbumin	14,178	60	$52 \times 32 \times 34$	−

*Molecular weight before labeling with Alexa fluor 633 (1089 Da).

[†]Diffusion coefficient D. Free Alexa fluor 633 C₅-maleimide: $D = 135$ $\mu m^2 s^{-1}$. Typical errors are mean ± SE 5%.

[‡]Dimensions of the macromolecules, based on the NMR and x-ray structures.

[§]Plus sign (+) indicates the substrate can efflux through MscL.

Purified MscL G22C was inserted into Triton X-100 destabilized liposomes as described (7,21). Briefly, 4 mg ml^{-1} liposomes were extruded 13× through 200-nm pore size polycarbonate filters (Avestin, Ottawa, Canada) and titrated with Triton X-100 until saturation. The lipid mixtures were composed of 1,2-dioleoyl-*sn*-glycero-3-phosphatidylcholine (DOPC), 1,2-dioleyl-*sn*-glycero-3-phosphatidylserine ((DOPS) Avanti Polar-Lipids, Alabaster, AL) and the fluorescent lipid analog 3,3′-dioctadecyloxacarbo-cyanine perchlorate ((DiO) Invitrogen, Carlsbad, CA; excitation and emission wavelengths of 484 and 499 nm, respectively) in a 30,000:10,000:1 mol ratio. MscL was added to the mixture in a protein to lipid ratio of ~1:50,000 (mol pentameric MscL/mol lipid) as estimated by a Folin reagent-based *DC*-protein assay (Bio-Rad, Hercules, CA). Subsequently, the detergent was removed by incubating the mixture overnight at 4°C with stepwise addition of 100 mg ml^{-1} Bio-Bead SM-2 polystyrene beads (Bio-Rad). Membrane reconstitution was performed in 50 mM potassium phosphate, pH 7.0.

Substrate labeling and encapsulation

To measure the upper size of molecules that can diffuse through MscL, several proteins were labeled with the fluorophore Alexa fluor 633 C5-maleimide (Invitrogen; excitation and emission of 621 and 639 nm, respectively). The hormone insulin from bovine pancreas (Sigma, St. Louis, MO), trypsin inhibitor from bovine pancreas (BPTI, Sigma), HPr of the phosphotransferase system (PTS) from *E. coli* (purified as described in Reizer et al. (20)), thioredoxin from *Spirulina* sp. (Sigma), and the calcium metalloprotein α-lactalbumin from bovine milk (Fluka, Milwaukee, WI) were labeled by adding 1 ml 100 μM protein solution in 30 mM K-Hepes, pH 8.5, to 40 nmol Alexa fluor 633, and the mixture was incubated for 30 min at room temperature. At this pH, maleimides not only react with sulfhydryl groups but also with primary amines such as the side chain of lysines and N-terminus of proteins. Reaction conditions (2.5-fold excess of protein over Alexa fluor 633; pH 8.5) were chosen to preferentially label the N-terminus. The buffer was exchanged to 50 mM potassium phosphate, pH 7.0 by gel filtration, using a Sephadex G-25 column (Nap10 column, Amersham Biosciences, Buckinghamshire, UK). Glutathione and the pep-tide RPPGFSPFC (bradykinin R9C, Genscript, Piscataway, NJ) were la-beled by adding 1 ml 500 μM solution in 50 mM potassium phosphate, pH 7.0, to 40 nmol Alexa fluor 633 C5-maleimide and incubating for 30 min at room temperature.

The Alexa fluor 633-labeled macromolecules were encapsulated into MscL-containing liposomes by at least three fast freezing (liquid nitrogen), and slow thawing (at 4°C) steps, at concentrations ranging from 1 to 10 μM and sample volumes of 200 μl. After this, 1 M of the membrane permeable osmolyte glycerol was added to slow down diffusion. The liposomes were extruded through 200 nm pore filters at a total lipid concentration of 2.5 mg ml^{-1}. The liposomes were diluted to a final concentration of 1 mg lipid ml^{-1} into 50 mM potassium phosphate, pH 7.0, plus 1 M glycerol in the presence or absence of 1 mM of either MTSET ([2-(trimethylammonium)ethyl] methanethiosulfonate bromide) or MTSES ([2-sulfonatoethyl] methanethio-sulfonate sodium salt, Anatrace, Maumee, OH) for opening of the MscL channels and incubated for 30 min at 18°C. FCS or fluorescence-burst analysis was then measured for 5–10 min at 18°C in a 2-μl volume.

Optical setup

Fluorescence-burst analysis and FCS measurements were carried out on a laser scanning confocal microscope (19), based on an inverted microscope Axiovert S 100 TV (Zeiss, Jena, Germany), in combination with a galva-nometer optical scanner (model 6860, Cambridge Technology, Watertown, MA) and a microscope objective nano-focusing device (P-721, PI). For excitation of the fluorescent lipid analog DiO, an argon ion laser (488 nm, Spectra-Physics, Irvine, CA) and for excitation of Alexa fluor 633 a He-Ne laser (633 nm, JDS Uniphase, Milpitas, CA) were focused by a Zeiss C-Apochromat infinity-corrected 1.2 N.A. 63× water immersion objective. The laser power for both channels did not exceed 10 μW at the back

aperture. Emission was collected through the same objective, separated from the excitation beams by a beam pick-off plate (BSP20-A1, ThorLabs, Newton, NJ), and split into two channels by a dichroic beam splitter (585dcxr, Chroma Technology, Brattleboro, VT) and finally directed through emission filters (HQ 535/50 and HQ675/50, Chroma Technology) and pinholes (diameters of 30 μm) onto two avalanche photodiodes (SPCM-AQR-14, EG&G, Gaithersberg, MD). The fluorescence signals were digitized and auto- and cross-correlation curves were calculated using a multiple τ-algorithm. The autocorrelation curves were fitted with a two-step analytical model (Supplementary Material; (21)). For the fluorescence-burst analysis, the fluorescence count traces for both colors were recorded for >300 s with a binwidth of 1 μs.

The setup was calibrated by measuring the known diffusion coefficients of Alexa fluor 488 and 633 in water (Invitrogen; $D = 300$ μm^2 s^{-1}). The lateral radii ω_{xy}, defined as the point where the fluorescence count rate per molecule decreased e^2 times, for 488 and 633 nm excitation were 180 and 240 nm, respectively, corresponding to detection volumes of ~0.20 fl and ~0.45 fl. For the dual-color fluorescence-burst analysis, the overlap between the two focal volumes was optimized by maximizing the cross-correlation signal of a double-labeled, double-stranded oligonucleotide. For this, the oligonucleotides 5′-ATT ATT GAG TGG TCA CTT TAA A-3′ and 5′-TTT AAA GTG ACC ACT CAA TAA T-3′, labeled with Alexa fluor 488 and 633, respectively (Invitrogen), were boiled together for 5 min at a final concentration of 0.5 μM and subsequently slowly cooled to 4°C to allow annealing. Afterwards, 1 mM NaN$_3$ was added as a preservative.

Fluorescence-burst analysis

Fluorescence-burst analysis was used to probe efflux through MscL. First, Alexa fluor 633-labeled macromolecules were encapsulated in MscL containing liposomes labeled with a second fluorophore DiO. Then, the fluorescence bursts emerging from diffusion of the liposomes through the focal volume of the dual-color confocal laser-scanning microscope was measured (Fig. 1 c). For all the bursts in the DiO fluorescence above a certain offset, the area of the ith peak (L_i) was then calculated:

$$L_i = \frac{1}{t_2 - t_1} \int_{t_1}^{t_2} I_{DiO} dt, \quad (1)$$

where the fluorescence in the DiO channel I_{DiO} is above the offset between times t_1 and t_2 (Fig. 1 c). For the fluorescence in the Alexa fluor 633 channel I_{AF633}, the corresponding signal (S_i) was also calculated:

$$S_i = \frac{1}{t_2 - t_1} \int_{t_1}^{t_2} I_{AF633} dt. \quad (2)$$

Because the fluorescence intensities are linearly proportional to the number of molecules, the concentration of macromolecules in arbitrary units, C_{arb}, could now be calculated:

$$[C_{arb}]_i = \frac{S_i}{L_i^{\frac{3}{2}}}. \quad (3)$$

In Eq. 3, the signals are normalized because DiO is associated to the surface of the liposomes and Alexa fluor 633 is present inside the vesicles; as a function of liposome radius, L_i and S_i thus scale to the power 2 and 3, respectively. From C_{arb}, the average concentration over all the liposomes (C_{av}) could be calculated:

$$C_{av} = \frac{\sum_{i=1}^{N_L} [C_{arb}]_i}{N_L}, \quad (4)$$

with N_L corresponding to the number of bursts. In addition to C_{av}, the number of empty liposomes was also determined. A burst in the DiO count rate corresponded to an empty liposome, when a corresponding burst in the Alexa fluor 633 count rate was absent. The above analysis assumes that the liposome diameter is smaller than that of the observation volume and that

the observation volumes of the two channels spatially coincide. In general, both assumptions can be satisfied by a proper adjustment of the objective fill-factors of the excitation laser beams and the diameters of the confocal pinholes.

RESULTS

To assess the diffusion of macromolecules through MscL, MscL G22C was reconstituted in liposomes that were labeled with the fluorescent lipid analog DiO. A series of Alexa fluor 633-labeled macromolecules was encapsulated in the liposomes. SDS-PAGE gels of Alexa fluor 633-labeled insulin, BPTI, HPr, thioredoxin, and α-lactalbumin, are shown in Fig. 2, where the proteins are visualized by ultraviolet (UV) illumination or Coomassie brilliant blue (CBB) staining. All the tested macromolecules were present in a monomeric form (22–25), which was confirmed by FCS and size-exclusion chromatography (not shown). The oligomeric state of insulin depends on its concentration and is monomeric at the concentration used here (26).

For the dual-color fluorescence-burst analysis, the fluorescence intensity fluctuations resulting from the liposomes diffusing through the confocal volume was measured for 5–10 min. During this time, 100–1000 liposomes passed
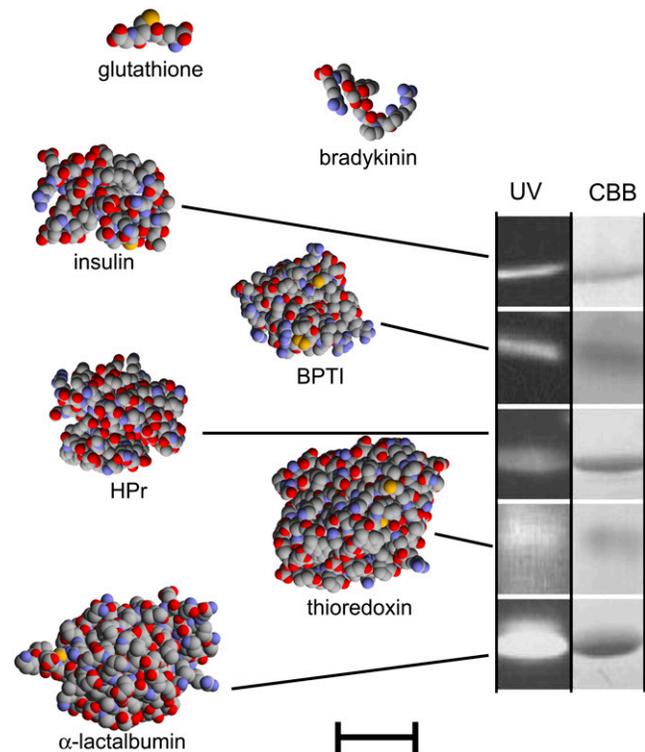
FIGURE 2 The size markers. SDS-PAGE gels after UV-illumination (UV) or Coomassie brilliant blue staining (CBB) of insulin, BPTI, HPr, thioredoxin, and α-lactalbumin, all labeled with Alexa fluor 633. The three-dimensional structures of the macromolecules encapsulated in the liposomes were taken from the RCSB protein data bank. Shown are the NMR structure of human insulin (38), and the x-ray structures of BPTI (39), HPr from E. coli (40), thioredoxin from E. coli (41), and human α-lactalbumin (42). The scale bar represents 2 nm.

through the focal volume, estimated from the fluorescence trace, where each burst corresponds to a liposome (Fig. 1 *c*). To verify whether the dual-color fluorescence-burst analysis was quantitative, Alexa fluor 633-labeled glutathione at 1, 5, and 10 μM was encapsulated inside liposomes containing DiO. The fluorescence intensities were accumulated for 10 min and the C_{arb}-values were calculated according to Eq. 3 (Fig. 3 *a*). The C_{av} values (Eq. 4) were 1.2 $\pm$ 0.3 for 1 μM, 3.8 $\pm$ 0.6 for 5 μM, and 7.9 $\pm$ 0.7 for 10 μM (Fig. 3 *b*), which is in fair agreement with the expected ratio of 1:5:10. The percentages of empty liposomes were 53 $\pm$ 12% for 1 μM, 24 $\pm$ 3% for 5 μM and 5.5 $\pm$ 1% for 10 μM (Fig. 3 *c*). These values are close to the values of 76%, 26%, and 6.6%, respectively, calculated from the average size of the liposomes (Supplementary Material), assuming a Poisson distribution of the number of molecules contained in the liposomes. Deviations between the measured and expected values are likely due to pipetting errors and uncertainties in the concentration of Alexa fluor 633-labeled glutathione, which were estimated from the absorption at 630 nm. Spatial differences in the observation volumes of the channels could also have contributed to the observed deviations.

The efflux from MscL-containing liposomes was studied by encapsulating Alexa fluor 633-labeled macromolecules; 4 μM glutathione, 8 μM insulin, 2 μM BPTI, 2 μM HPr, 2 μM thioredoxin, or 8 μM α-lactalbumin were encapsulated into the DiO-labeled liposomes. The mass of Alexa fluor 633 was determined to be 1089 Da using mass spectrometry (Supplementary Material). The macromolecules did not associate measurably with the membrane, as was verified by the addition of the Alexa fluor 633-labeled macromolecules to DiO containing liposomes and performing dual-color fluorescence-burst analysis (data not shown). The complete histograms of BPTI and thioredoxin are shown in Fig. 4, *a* and *b*. Fig. 4 *c* shows the average concentration C_{av} of the tested compounds in the liposomes, and Fig. 4 *d* shows the percentages of empty liposomes. Upon opening of the MscL G22C channel by modification with MTSET or MTSES, the concentration of glutathione, insulin, and BPTI decreased significantly, whereas in the case of HPr, thioredoxin, and α-lactalbumin there was no significant change (Fig. 4 *c*). Furthermore, the fraction of empty liposomes increased for

glutathione from 37.5 $\pm$ 0.5% to 62 $\pm$ 5%, for insulin from 11 $\pm$ 2% to 36 $\pm$ 2%, and for BPTI from 54.5 $\pm$ 2% to 71.5 $\pm$ 2%. In the case of insulin and BPTI, modification of MscL with the negatively charged MTSES resulted in an increase of empty liposomes comparable to MTSET. When HPr, thioredoxin, or α-lactalbumin were incorporated into liposomes, there was no increase in the fraction of empty liposomes upon MscL-modification with either MTSET or MTSES (Fig. 4 *d*). Addition of MTSET and MTSES to the labeled macromolecules in solution did not result in a change in fluorescence. Furthermore, MTSET and MTSES did not affect efflux of Alexa fluor 633-labeled glutathione or BPTI, encapsulated in liposomes without MscL, indicating that efflux occurred through MscL. Finally, steady-state levels of efflux were reached and the liposomes were not leaky due to, for instance, residual detergent, since the concentration distributions were stable for >24 h.

To verify the results obtained by dual-color fluorescence-burst analysis, the diffusion of macromolecules was assessed using FCS. With FCS, one can determine diffusion constants and concentrations (21) for ensemble averages and not individual particles as with dual-color fluorescence-burst analysis. The fluorescence autocorrelation signals of the DiO and the Alexa fluor 633 channels were measured and the data were fitted with a two-step analytical model to quantify the release of macromolecules (Supplementary Material). In the case of glutathione, the nonameric peptide bradykinin R9C, insulin, and BPTI, opening of the channel resulted in an increase of the fraction of fast component *F*, which corresponds to the released fluorophore (Fig. 5). No increase was observed for HPr, thioredoxin, and α-lactalbumin. These results are in perfect agreement with the results obtained by the dual-color fluorescence-burst analysis. The fluorescence-burst analysis, however, has the advantage over FCS of yielding a distribution of macromolecules over the liposomes, whereas FCS only provides qualitative information.

DISCUSSION

Both dual-color fluorescence-burst analysis and FCS revealed that the tripeptide glutathione, the nonameric peptide bradykinin R9C, insulin, and BPTI, all labeled with Alexa
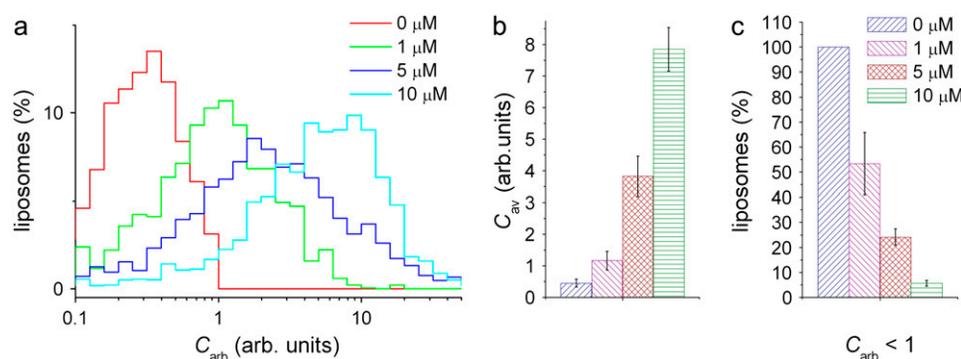
FIGURE 3 Dual-color fluorescence-burst analysis: proof of principle. (*a*) Histogram shows the distribution of liposomes loaded with 0, 1, 5, or 10 μM of glutathione as a function of C_{arb} (Eq. 3). (*b*) The average concentration C_{av} (Eq. 4) of the Alexa fluor 633-labeled molecules in the liposomes. (*c*) The percentages of empty liposomes. Error bars were calculated from three measurements.
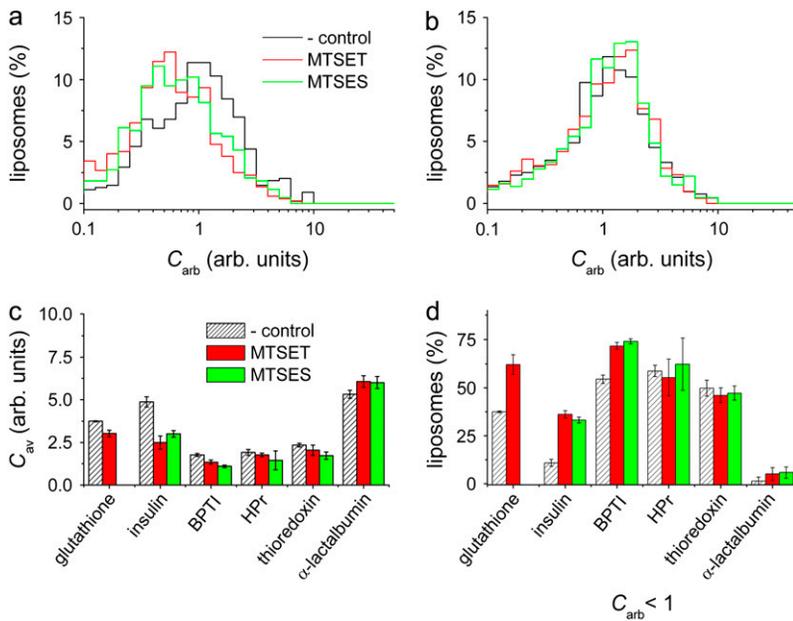
FIGURE 4 Dual-color fluorescence-burst analysis: protein passage through MscL. Histogram shows the distribution of MscL G22C containing liposomes loaded with (*a*) 2 μM BPTI and (*b*) 2 μM thioredoxin, unmodified (control) or modified with MTSET or MTSES, as a function of C_{arb} (Eq. 3). (*c*) The average concentration C_{av} of the Alexa fluor 633-labeled molecules in the liposomes (Eq. 4). (*d*) The percentages of empty liposomes. Error bars were calculated from three measurements.

fluor 633, are able to efflux through MscL, whereas HPr, thioredoxin, and α-lactalbumin are not. The molecular weights and dimensions of these macromolecules, derived from the three-dimensional structures and presented by the Research Collaboration for Structural Bioinformatics Protein Data Bank ((RCSB PDB); Fig. 2), are given in Table 1. These dimensions do not include the bound Alexa fluor 633 label of 1089 Da. As a result of this labeling, the dimensions of glutathione and bradykinin are dominated by the Alexa fluor 633 label. Because of the dimensions of insulin and BPTI (Table 1), the diameter of MscL must be larger than ~3 nm. This diameter holds for MscL opened by MTSES or MTSET, which bind a moiety of ~5–6 Å to each of the subunits of the channel (16) in an unknown conformation. Patch-clamp experiments showed that the conductances of MscL channels opened by modification with MTSET and opened by stretching of the membrane by a negative pipette pressure are comparable (16), suggesting a similar pore diameter. The pore diameter estimated from the passage of insulin and BPTI is consistent with calculated estimates of 29–46 Å based on the conductance of the channel (11,12).

It has been suggested that some small organic osmolytes like ATP, glycine betaine, and trehalose are hindered in their diffusion through MscL (27). In view of the data presented here on protein efflux, and reports on fluorophore (6,8) and glycine betaine efflux via MscL (28), the earlier claims that cytoplasmic molecules are rejected from entering the pore (5,27) seem questionable. It is possible, however, that the rates at which different types of molecules diffuse through MscL vary greatly. Owing to the limited time resolution of the dual-color fluorescence-burst analysis, we could not obtain kinetic information on (macro)molecule diffusion through the pore. The reason is that liposomes diffuse very slow due to their relatively large size. The measured average diffusion

speed of liposomes (γ/R, Eq. 5) is ~60 times smaller than that of free Alexa 633 dye. To measure enough liposomes to obtain an acceptable autocorrelation curve, the measurement time should typically be >1 min and information about rates of diffusion are not readily obtained. Thus, the diffusion through MscL of gluthathione, bradykinin, insulin, and BPTI (and possibly that of ATP; (27)) may be slow compared to that of ions.

It has been proposed (27) that the S3 domain of the associated C-terminal helices of the MscL pentamer forms a prefilter for metabolites at the cytoplasmic entrance, excluding high-molecular weight substances from entering the pore. We clearly show that macromolecules up to at least 6.5 kDa can pass through MscL, but we cannot distinguish between the prefilter or the actual pore in determining the size exclusion limits of the channel. Efflux experiments with the Δ110–136 mutant, lacking this S3 domain (29), might elucidate the role of the S3 domain in determining the pore size. It has been claimed (5) that wild-type *E. coli* cells release thioredoxin upon an osmotic downshift, whereas thioredoxin is retained by $mscL^{-}$ cells, suggesting that thioredoxin is able to diffuse through MscL. This observation contradicts our work. Our estimates should be regarded as lower limits, because proteins may be hindered in their passage due to binding to the surface of the pore or interaction with the methanethiosulfonate label. We consider the latter less probable because MscL modification with positively charged (MTSET) and negatively charged (MTSES) labels yielded identical results. Lastly, our pore diameter matches the value obtained by patch-clamp studies, where it was found that poly-L-lysines with a diameter >37 Å blocked the conductance of the channel, whereas smaller poly-L-lysines had no effect (11).

The 52-kDa elongation factor Tu, the 41-kDa heatshock protein DnaK, and the 142-kDa enterobactin synthase
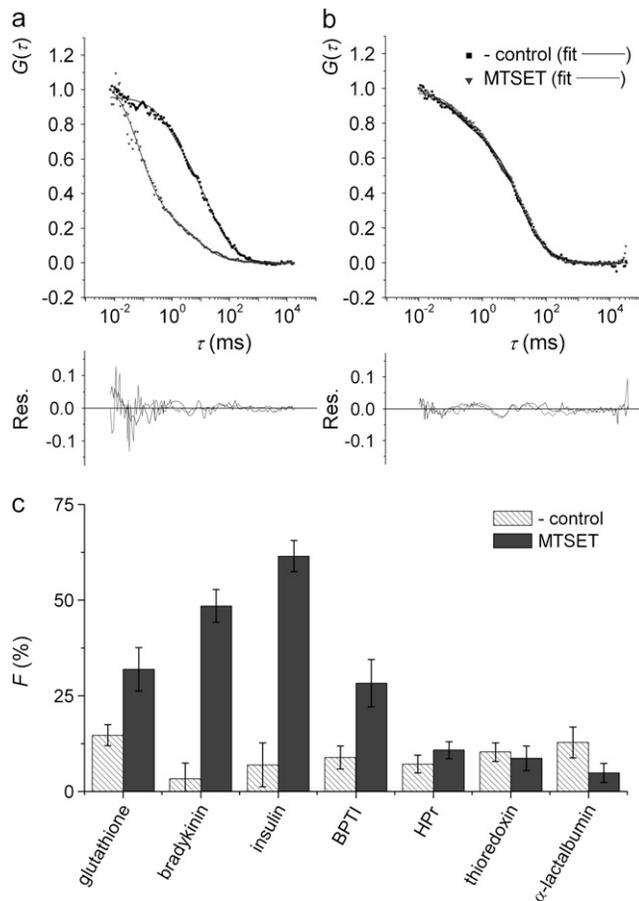
FIGURE 5 FCS measurements. Fluorescence autocorrelation curves of MscL containing liposomes, before (*black line/squares*) and after (*gray line/triangles*) opening of the channel by modification with MTSET. Shown are typical autocorrelation measurements for liposomes containing (*a*) insulin and (*b*) thioredoxin, both labeled with Alexa fluor 633. Curves were fitted with a two-step analytical model (Supplementary Material) and residuals are shown (*Res*). (*c*) The percentage of particles with a high mobility (*F*), corresponding to released substrates, of all tested macromolecules. Error bars were calculated from three measurements.

polypeptide EntF have been reported to be released upon osmotic downshock (13–15), and these macromolecules have been hypothesized to pass through MscL. Due to the high molecular weight and large dimensions of these molecules, this seems rather unlikely. Moreover, a more recent study with a MscL knockout strain suggests that these molecules might be released via a mechanism independent of MscL (4). The genome of *E. coli* K12 contains 262 open reading frames coding for proteins <9.2 kDa, of which 46 are predicted transmembrane proteins and 26 are secreted proteins. Of the remaining 190 open reading frames, >100 are proteins of unknown functions and for a large number it is not known whether they self-associate or complex with other proteins. Therefore, the number of proteins, potentially able to diffuse through MscL upon an osmotic downshift, will most likely be <100. Nevertheless, the release of this relatively small number of proteins could be physiologically significant.

Efflux through MscL was previously assessed by two techniques: patch-clamp and calcein dequenching (8,11,16). Both methods have a number of limitations compared to the fluorescence-based approach used in this work. In the case of the patch-clamp technique, direct translocation of proteins through membrane pores is not readily observed because of limited charges on the proteins relative to the free ions in the solution. Protein translocation, however, can be observed indirectly through blocking of the channel conductance (11,30,31). The calcein efflux assay is based upon the self-quenching of fluorophore (8) at very high concentrations (typically 25–100 mM), unlike the low concentrations used here (1–10 μM). Because fluorophore-labeled proteins cannot be incorporated at concentrations needed for self-quenching, calcein dequenching is not feasible for monitoring efflux of macromolecules. The fluorescence-based approach used in this work has further advantages of relatively short measurement times (typically 5 min) and small volumes ($\sim$1 μl). In this study, the diffusion through MscL was studied both by dual-color fluorescence-burst analysis and FCS. The FCS results, however, provide no information on the distribution of the macromolecules over the liposomes.

Similar to the fluorescence-based techniques used in this study, the macromolecule efflux from liposomes could also be studied with size exclusion chromatography. However, such measurements do not yield information on the distribution of macromolecules over the liposomes. Furthermore, much more material ($\sim$100$\times$) is needed for size exclusion chromatography. In addition to fluorescence autocorrelation spectroscopy, efflux could be measured using dual-color fluorescence cross-correlation spectroscopy (32), since DiO and the Alexa fluor 633-labeled macromolecules have distinctive emission and excitation wavelengths. However, according to our experience, the cross-correlation curve is difficult to quantify and prone to substantial errors because a large fraction of the liposomes does not contain an active channel or labeled macromolecule. Thus, the change of the cross-correlation curve upon opening of the channels is small. Therefore, in this particular case, dual-color fluorescence cross-correlation spectroscopy is expected to be less accurate than fluorescence autocorrelation spectroscopy.

Using fluorescence-burst analysis, it was shown that after opening of the channels, a large fraction of the liposomes still contained the same concentration of fluorescent-labeled macromolecule as before opening, even in the case of glutathione, insulin, and BPTI, which were able to diffuse through MscL. This indicates that a large fraction (between 40 and 70%) of the liposomes did not contain a functional MscL channel. Based on the reconstitution ratio of MscL pentamer/lipid of 1:50,000 (mol/mol), it is expected that each liposome should contain $\sim$10 MscL channels. Because about half of the liposomes did not contain an active channel, $\sim$90% of the channel must have been lost during the reconstitution and/or not functionally incorporated into the liposomes. This agrees with the reconstitution efficiencies reported

in the literature. For instance, for MscL pentamer/lipid ratios of from 1:50,000 to 1:10,000 (mol/mol) typically only one to seven active channels are found in a patch with a diameter of $\sim 1 \mu m$, instead of the expected 30–150 (8,33,34). On the basis of thiol-labeling with membrane-impermeant reagents, the majority of "active" MscL seems to be oriented right-side-in, but always a fraction of inside-out protein is present ((35); A. Kocer, Biomade Technology Foundation, personal communication, 2006). When these preparations were frozen-thawed up to eight times, we did not see a change in the efflux activity (or specificity) (G. van den Bogaart, unpublished data). Although these data are consistent with the notion that MscL is active in both orientations, it was technically not possible to rule out the possibility that protein efflux occurred via the fraction of inside-out oriented molecules.

In conclusion, this is the first time that efflux of macromolecules through MscL has been unequivocally demonstrated. Dual-color fluorescence-burst analysis provides an approach of analyzing the permeability properties of membrane proteins, with a number of merits compared to existing methods. It can be used as a universal method to study translocation of fluorophore-labeled macromolecules by membrane pores, expressed in cells or reconstituted in liposomes. The method should be also of particular importance for studying the effective pores of antimicrobial peptides, for which channel formation and membrane permeabilization is still elusive (36,37). Preliminary experiments have demonstrated the usefulness of fluorescence-burst analysis in determining the pore properties of magainin 2, melittin, and indolicidin (G. van den Bogaart and J. Mika, unpublished data).

SUPPLEMENTARY MATERIAL

An online supplement to this article can be found by visiting BJ Online at http://www.biophysj.org.

REFERENCES

1. Sukharev, S. I., P. Blount, B. Martinac, F. R. Blattner, and C. Kung. 1994. A large-conductance mechanosensitive channel in *E. coli* encoded by MscL alone. *Nature*. 368:265–268.

2. Nossal, N. G., and L. A. Heppel. 1966. The release of enzymes by osmotic shock from Escherichia coli in exponential phase. *J. Biol. Chem.* 241:3055–3062.

3. Schleyer, M., R. Schmid, and E. P. Bakker. 1993. Transient, specific and extremely rapid release of osmolytes from growing cells of *Escherichia coli* K-12 exposed to hypoosmotic shock. *Arch. Microbiol.* 160:424–431.

4. Vázquez-Laslop, N., H. Lee, R. Hu, and A. A. Neyfakh. 2001. Molecular sieve mechanism of selective release of cytoplasmic proteins by osmotically shocked *Escherichia coli*. *J. Bacteriol.* 183:2399–2404.

5. Ajouz, B., C. Berrier, A. Garrigues, M. Besnard, and A. Ghazi. 1998. Release of thioredoxin via mechanosensitive channel MscL during osmotic downshock of *Escherichia coli* cells. *J. Biol. Chem.* 273: 26670–26674.

6. Smisterova, J., M. van Deemter, G. van der Schaaf, W. Meijberg, and G. Robillard. 2005. Channel protein-containing liposomes as delivery vehicles for the controlled release of drugs-optimization of the lipid composition. *J. Controlled Release*. 101:382–383.

7. Folgering, J. H. A., J. M. Kuiper, A. H. de Vries, J. B. F. N. Engberts, and B. Poolman. 2004. Lipid-mediated light activation of a mechanosensitive channel of large conductance. *Langmuir*. 20:6985–6987.

8. Koçer, A., M. Walko, W. Meijberg, and B. L. Feringa. 2005. A light-actuated nanovalve derived from a channel protein. *Science*. 309: 755–758.

9. Sukharev, S., M. Betanzos, C. Chiang, and H. R. Guy. 2001. The gating mechanism of the large mechanosensitive channel MscL. *Nature*. 409:720–724.

10. Folgering, J. H. A., J. C. Wolters, and B. Poolman. 2005. Engineering covalent oligomers of the mechanosensitive channel of large conductance from *Escherichia coli* with native conductance and gating characteristics. *Protein Sci.* 14:2947–2954.

11. Cruickshank, C. C., R. F. Minchin, A. C. Le Dain, and B. Martinac. 1997. Estimation of the pore size of the large-conductance mechanosensitive ion channel of *Escherichia coli*. *Biophys. J.* 73:1925–1931.

12. Sukharev, S. I., W. J. Sigurdson, C. Kung, and F. Sachs. 1999. Energetic and spatial parameters for gating of the bacterial large conductance mechanosensitive channel, MscL. *J. Gen. Physiol.* 113:525–540.

13. Hantash, F. M., M. Ammerlaan, and C. F. Earhart. 1997. Enterobactin synthase polypeptides of *Escherichia coli* are present in an osmotic-shocksensitive cytoplasmic locality. *Microbiology*. 143:147–156.

14. Berrier, C., A. Garrigues, G. Richarme, and A. Ghazi. 2001. Elongation factor Tu and DnaK are transferred from the cytoplasm to the periplasm of *Escherichia coli* during osmotic downshock presumably via the mechanosensitive channel MscL. *J. Bacteriol.* 182: 248–251.

15. Jacobson, G. R., B. J. Takacs, and J. P. Rosenbusch. 1976. Properties of a major protein released from *Escherichia coli* by osmotic shock. *Biochemistry*. 15:2297–2303.

16. Yoshimura, K., A. Batiza, and C. Kung. 2001. Chemically charging the pore constriction opens the mechanosensitive channel MscL. *Biophys. J.* 80:2198–2206.

17. Blount, P., S. I. Sukharev, P. C. Moe, M. J. Schröder, H. R. Guy, and C. Kung. 1996. Membrane topology and multimeric structure of a mechanosensitive channel protein of Escherichia coli. *EMBO J.* 15: 4798–4805.

18. Ou, X., P. Blount, R. Hoffman, and C. Kung. 1998. One face of a transmembrane helix is crucial in mechanosensitive gating. *Proc. Natl. Acad. Sci. USA*. 95:11471–11475.

19. Doeven, M. K., J. H. Folgering, V. Krasnikov, E. R. Geertsma, G. van den Bogaart, and B. Poolman. 2005. Distribution, lateral mobility and function of membrane proteins incorporated into giant unilamellar vesicles. *Biophys. J.* 88:1134–1142.

20. Reizer, J., S. L. Sutrina, L. F. Wu, J. Deutscher, P. Reddy, and M. H. Saier Jr. 1992. Functional interactions between proteins of the phosphoenolpyruvate: sugar phosphotransferase systems of *Bacillus subtilis* and *Escherichia coli*. *J. Biol. Chem.* 267:9158–9169.

21. Rigler, R., Ü. Mets, J. Widengren, and P. Kask. 1993. Fluorescence correlation spectroscopy with high count rate and low background: analysis of translational diffusion. *Eur. Biophys. J.* 22:169–175.

22. Hammen, P. K., E. B. Waygood, and R. E. Klevit. 1991. Reexamination of the secondary and tertiary structure of histidine-containing protein from *Escherichia coli* by homonuclear and heteronuclear NMR spectroscopy. *Biochemistry*. 30:11842–11850.

23. Carulla, N., C. Woodward, and G. Barany. 2000. Synthesis and characterization of a beta-hairpin peptide that represents a 'core module' of bovine pancreatic trypsin inhibitor (BPTI). *Biochemistry*. 39:7927–7937.

24. Reutimann, H., B. Straub, P. L. Luisi, and A. Holmgren. 1981. A conformational study of thioredoxin and its tryptic fragments. *J. Biol. Chem.* 256:6796–6803.

25. Hill, R. L., K. Brew, T. C. Vanaman, I. P. Trayer, and P. Mattock. 1968. The structure, function, and evolution of alpha-lactalbumin. *Brookhaven Symp. Biol.* 21:139–154.

26. Jeffrey, P. D., and J. H. Coates. 1966. An equilibrium ultracentrifuge study of the self- association of bovine insulin. *Biochemistry.* 5:489–498.

27. Anishkin, A., V. Gendel, N. A. Sharifi, C. S. Chiang, L. Shirinian, H. R. Guy, and S. Sukharev. 2003. On the conformation of the COOH-terminal domain of the large mechanosensitive channel MscL. *J. Gen. Physiol.* 121:227–244.

28. Folgering, J. H. A., P. C. Moe, G. K. Schuurman-Wolters, P. Blount, and B. Poolman. 2005. *Lactococcus lactis* uses MscL as its principal mechanosensitive channel. *J. Biol. Chem.* 280:8784–8792.

29. Blount, P., S. I. Sukharev, M. J. Schroeder, S. K. Nagle, and C. Kung. 1996. Single residue substitutions that change the gating properties of a mechanosensitive channel in *Escherichia coli*. *Proc. Natl. Acad. Sci. USA.* 93:11652–11657.

30. Krantz, B. A., L. Sachs, B. M. Ahlberg, P. Nordin, and T. Nilstun. 2005. A phenylalanine clamp catalyzes protein translocation through the anthrax toxin pore. *Science.* 309:777–781.

31. Movileanu, L., J. P. Schmittschmitt, J. M. Scholtz, and H. Bayley. 2005. Interactions of peptides with a protein pore. *Biophys. J.* 89:1030–1045.

32. Schwille, P., F. J. Meyeralmes, and R. Rigler. 1997. Dual-color fluorescence cross-correlation spectroscopy for multicomponent diffusional analysis in solution. *Biophys. J.* 72:1878–1886.

33. Moe, P., and P. Blount. 2005. Assessment of potential stimuli for mechano-dependent gating of MscL: effects of pressure, tension, and lipid headgroups. *Biochemistry.* 44:12239–12244.

34. Hase, C. C., A. C. Le Dain, and B. Martinac. 1995. Purification and functional reconstitution of the recombinant large mechanosensitive ion channel (MscL) of *Escherichia coli*. *J. Biol. Chem.* 270:18329–18334.

35. Koçer, A., M. Walko, E. Bulten, E. Halza, B. L. Feringa, and W. Meijberg. 2006. Rationally designed chemical modulators convert a bacterial channel protein into a pH-sensory valve. *Angew. Chem. Int. Ed. Engl.* 45:3126–3130.

36. Brogden, K. A. 2005. Antimicrobial peptides: pore formers or metabolic inhibitors in bacteria? *Nat. Rev. Microbiol.* 3:238–250.

37. Toke, O. 2005. Antimicrobial peptides: new candidates in the fight against bacterial infections. *Biopolymers.* 80:717–735.

38. Ludvigsen, S., H. B. Olsen, and N. C. Kaarsholm. 1998. A structural switch in a mutant insulin exposes key residues for receptor binding. *J. Mol. Biol.* 279:1–7.

39. Parkin, S., B. Rupp, and H. Hope. 1996. Structure of bovine pancreatic trypsin inhibitor at 125 K definition of carboxyl-terminal residues Gly57 and Ala58. *Acta Crystallogr. D Biol. Crystallogr.* 52:18–29.

40. Napper, S., L. T. J. Delbaere, and E. B. Waygood. 1999. The aspartyl replacement of the active site histidine-containing protein, HPr, of the *Escherichia coli* phosphoenolpyruvate: sugar phosphotransferase system can accept and donate a phosphoryl group. Spontaneous dephosphorylation of acyl-phosphate autocatalyzes an internal cyclization. *J. Biol. Chem.* 274:21776–21782.

41. Lennon, B. W., C. H. Jr. Williams, and M. L. Ludwig. 1999. Crystal structure of reduced thioredoxin reductase from *Escherichia coli*: structural flexibility in the isoalloxazine ring of the flavin adenine dinucleotide cofactor. *Protein Sci.* 8:2366–2379.

42. Chandra, N., K. Brew, and K. R. Acharya. 1998. Structural evidence for the presence of a secondary calcium binding site in human α-lactalbumin. *Biochemistry.* 37:4767–4772.